

Mineralogical study of the triassic clay of Maaziz and the Pliocene Marl of Akrach in Morocco: Characterization and preliminary study for evaluating the potential use of these geomaterials in traditional ceramics

Sahar El Kasmi^{1*}, Ayoub Aziz², Boubker Boukili¹, Nacir El Moutaouakkil¹, M'hamed El Janati¹, Mohammed Saadi¹, Chol Lucka Awan¹, Imane Kounti¹

¹Faculty of Sciences, Mohammed V University Av, Ibn Batouta BP1014 Agdal, Rabat, Morocco; s.elkasmi@um5r.ac.ma (S.E.K.) b.boukili@um5r.ac.ma (B.B.) n.elmoutaouakkil@um5r.ac.ma (N.E.M.) m.eljanati@um5r.ac.ma (M.E.J.) m-saadi@um5r.ac.ma (M.S.) imanekounti1994@gmail.com (I.K.) chol.mayom@um5r.ac.ma (C.L.A.)

²Scientific Institute of Rabat, Mohammed V University, Av Ibn Battuta BP1014 Agdal, Rabat, Morocco; ayoub_aziz2@um5r.ac.ma (A.A.)

Abstract: This study was conducted as a multidisciplinary collaboration between geologists, chemists, and industrial ceramics. Two main sites were identified for the collection of geological raw materials, to study the relationship between the mineralogy of clays and some physical parameters of finished ceramic pieces (such as porosity density and absorption.). A protocol was developed to study raw clay samples of Triassic clay and Pliocene marl acquired from the Maaziz and Akrach regions, respectively, in northeast Morocco. The process involved sampling from the sources, as well as mineralogical and physicochemical characterizations. The raw materials were characterized using X-ray diffraction spectrometry (XRD), infrared (IR) spectroscopy, and X-ray fluorescence spectroscopy (FX), making it possible to determine the structure and nature of clay. The obtained specimens—90%, 80%, and 70% Triassic clay or 10%, 20%, and 30% Pliocene marl—contribute to the balancing of raw clays and lead to a marked improvement in the quality of ceramic products, including a reduction in their firing shrinkage and an increase in flexural strength. The results indicated that the incorporation of Pliocene clay reduced the risk of fracture of the Triassic clay, with a noticeable reduction observed at 10% addition. No fractures were observed when 20% and 30% Pliocene clay was added. These findings suggest that Pliocene clay can enhance the mechanical properties and structural integrity of Triassic clay-based products.

Keywords: Akrach region, Geomaterials, Maaziz region, Mineralogical composition, Morocco, Pliocene clay, Traditional ceramic, Triassic clay.

1. Introduction

The Rabat-Salé-Kénitra region of Morocco is a treasure trove of cultural heritage and historical significance [1][2]. Baked clay (pottery) has played a vital role in artistic expression, architectural design, and functional applications for centuries. By understanding the characteristics of the local clay and traditional ceramic practices, we can gain valuable insights into the cultural heritage and technological advancements of this region [3][4]. The use of clay and ceramics in the Rabat-Salé-Kénitra region dates back to ancient times. The region's rich clay deposits have been utilized by local artisans and craftsmen to create a wide range of ceramic products, including pottery, tiles, and architectural elements. These ceramics not only served functional purposes but also showcased the artistic skills and cultural identity of the people. To gain a deeper understanding of the clay and ceramics in this region, a bibliographic analysis was conducted. This involved studying various scholarly articles, books, and research papers that focused on the subject. The analysis revealed that clay in the

Rabat-Salé-Kénitra region is known for its high plasticity and fine particle size, making it ideal for shaping and molding. Several trials were undertaken to examine the characteristics of ceramics made from two specific clay types: Triassic clay from the Maaziz region and Pliocene marl from the Akrach region. Triassic clay is known for its reddish-brown color, which gives the ceramics a distinct earthy tone. Miocene marl, on the other hand, is characterized by its grayish-yellow color and lower iron content, resulting in ceramics with a lighter appearance [5] [6].

The present paper tackles various topics related to the uses of baked clay in the study region, such as pottery. It aims to highlight the mineralogy of Triassic clays from the Maaziz region and Miocene marls from the Akrach area, as well as the potential applications of traditional ceramics produced from these materials. Therefore, it seemed interesting to evaluate the effect of thermal treatment on certain parameters such as the porosity, density, absorption, and color of the different ceramic samples made from these two natural materials [7].

This knowledge can guide artisans in the region, especially since firing techniques play a crucial role in the transformation of clay into ceramics. By understanding the optimal firing conditions and physical properties of these clays, artisans can enhance the quality of their ceramic products and make informed decisions regarding their manufacturing processes [8].

Additionally, the study may lead to recommendations for specific applications based on the mineralogical properties of each clay type. This can enhance local ceramic practices and contribute to a broader understanding of the use of geomaterials in this region, particularly Triassic clays and Miocene marls [9].

2. Materials and Methods

2.1. Geological Setting

Two main sites were identified for the collection of the geological raw materials Triassic clay and Pliocene clay, sourced from the Maaziz and Akrach regions, respectively, as shown on the map below (Figure 1).

The two outcrops selected for sampling were chosen over other equivalent Triassic and Pliocene clay deposits due to their geological significance and considerations of access and logistics. Indeed, these sites exhibit unique geological characteristics that are representative of the Triassic and Pliocene periods, particularly in terms of stratigraphy. For example, the well-preserved stratigraphy of these outcrops allows for a better understanding of the geological evolution of the region. Additionally, the accessibility of these sites facilitates fieldwork and sample collection, which are essential for ensuring the quality of the analyses. By combining their geological relevance with practical considerations, we have selected locations that optimize both the richness of scientific data and the feasibility of the research.

The Triassic outcrop has never been subjected to any previous mineralogical characterization studies.

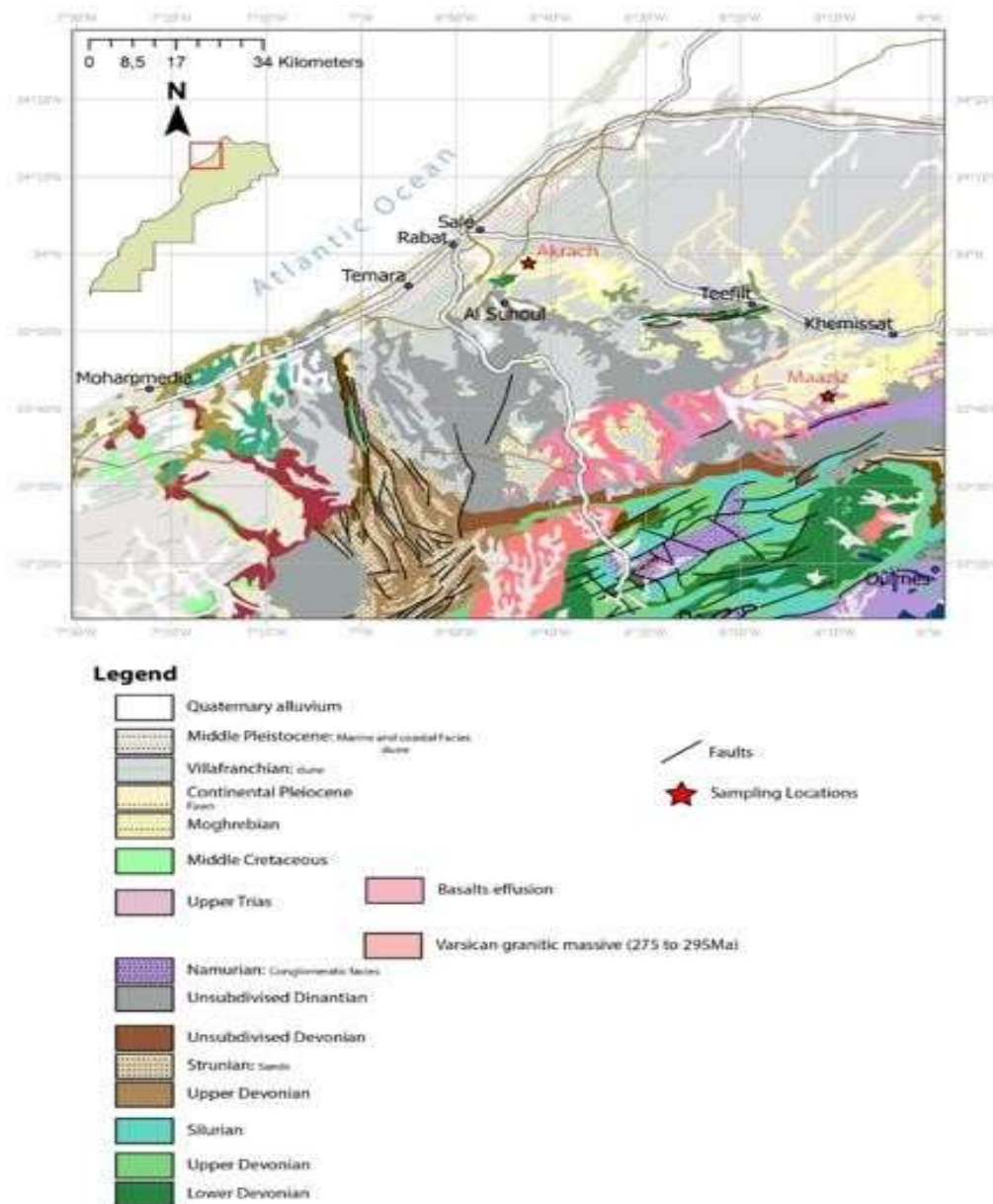


Figure 1.
Digital map showing geographical location of the studied sampling (ArcGis).

Figure 1 shows the geographical area covered by the study's two regions of concern.

The Akrach area, which is located in a Pliocene marine basin and is part of the southern Rifain trough, corresponds to a tectonic weak zone. The collapse of this zone creates a basin that serves as a receptacle for enormous inputs of clays and sands. The sedimentary formations are characterized by three main layers of respective ages: Miocene, Pliocene, and Quaternary (Fig.2b) [10]. The Maaziz area is located in the northwest of Morocco, 96 km east of Rabat, and is part of the Triassic basin of Khemisset (Fig. 2a) [11]. In general terms, this Triassic basin belongs to the central massif of the Moroccan meseta and is presented as a half-graben of NE–SW orientation, boxed between two Hercynian moles: the anticlinorium of Khouribga-Oulmès in the southeast and the anticlinorium of Tiflet to the northwest. The Triassic deposits outcrop in the northwest and southwest part of the city of Maaziz is covered by

the Mio-Pliocene deposits towards the northeast. They are surmounted concordantly by a red layer attributed to the Lias (Lower Jurassic) in places or directly by the marls and conglomerates of the Pliocene.

The geodynamic evolution of the Triassic basins is part of the opening of the Atlantic during the Upper Triassic and the Lower Liassic [Hassan E et al., 2014]. It takes up the Hercynian structural heritage and is completed by all the syn and post-rift events that have intervened for the structuring of the Triasico-liassic basins [12].

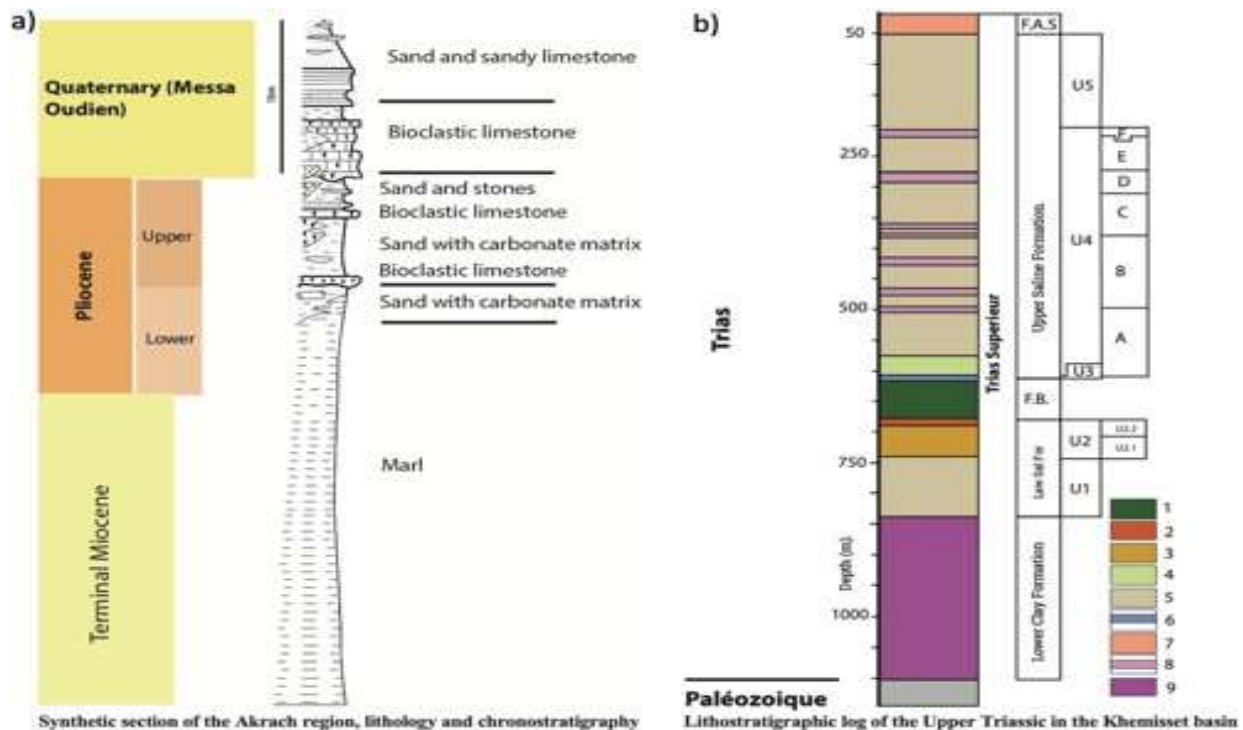


Figure 2. General stratigraphic logs of the studied sections (a) from the Akraich region [10] and (b) from the Maaziz region [11] [13].

By utilizing geological mapping in conjunction with lithological sections, we aimed to achieve a more comprehensive analysis of the geological characteristics of the region. While common geological maps provide a valuable overview of an area's geology, lithological sections allow for a more nuanced examination of the data. For example, they present the thickness of the Triassic and Miocene layers, highlighting their significance in terms of clay potential and enabling us to identify specific characteristics and patterns that may not be readily apparent on a standard map. This approach enhances our ability to select the most representative sampling points by integrating quantitative data with geological insights.

2.2. Experiments

2.2.1. Apparatus

We applied spectral classification algorithms in ENVI to delineate clay zones in our study area (Rabat-Salé-Kénitra region), utilizing ASTER (Advanced Spaceborne Thermal Emission and Reflection Radiometer) data. The ASTER images were radiometrically and atmospherically corrected to remove atmospheric effects and normalize the data. Previous studies have demonstrated the effectiveness of this approach. For instance, Mashimbye et al. (2012) used ASTER data and ENVI software to map clay zones in the Limpopo region of South Africa [14], achieving notable success in identifying specific types of

clays. Rowan and Mars (2003) illustrated the use of ASTER data for mapping hydrothermal minerals in the Mojave Desert of California [15].

When using ASTER data for regional-scale mineral or lithological mapping, it is important to consider several aspects. Primarily, cloud cover, vegetation, and atmospheric effects can significantly bias the surface reflectance recorded by the sensor. Additionally, band ratios do not definitively indicate the presence of a mineral. Moreover, each terrain type is unique, so band ratios that work in some areas for a specific mineral or assemblage may not show the same results elsewhere. The results have a more qualitative than quantitative nature, so ground truthing is essential and it is important to consider ASTER images in combination with other data. Datasets such as geological maps, geochemistry, ground spectral measurements, and any other available data should be used in conjunction with ASTER data to enable the most accurate interpretation.

Mineralogical characterization was performed using X-ray diffraction (XRD). The patterns were recorded in a PANalytical diffractometer Model PW3040/60 X'pert PRO operating with Cu K α radiation (K α 0.15406 nm) generated at 40 kV and 20 mA. Scans were carried out at

0.02 °min⁻¹ for 2 θ values between 3 and 40. The infrared (IR) spectra of clay samples mixed with KBr were recorded with a vertex 70 spectrophotometer, operating in the range 4000–400 cm⁻¹. Also, X-ray fluorescence (FX) tests were carried out, using a Wavelength Dispersion Spectrometer of the Axios Type for the chemical characterization of clay.

The fabrication of ceramic bricks involves a variety of specialized materials and equipment, each serving a critical function in the production process. The drying and heating chamber was essential for removing moisture from the collected clay materials at a set temperature of 105 °C, ensuring they achieved optimal strength during firing. A grinding and mixing machine, such as the Planetary Ball Mill, plays a vital role in achieving a homogeneous mixture of raw materials by finely grinding and thoroughly blending them. To maintain the quality of the mixture, a Vibratory Sieve Shaker was employed to eliminate lumps and foreign particles, ensuring a consistent texture. Precision is key, which is why an Analytical Balance was utilized for accurate measurement of the ingredients, adhering to specific formulation requirements. The brick molding machine efficiently shaped the mixed clay into uniform blocks, facilitating the production process. Additionally, a modifier was sprayed onto the mixed clay to adjust its plasticity, making it easier to mold and shape by enhancing its workability. Finally, the Vulcan A-130 Lab Furnace, capable of reaching high temperatures, was crucial for the final firing of the bricks as it solidified their structure and enhanced durability. Together, these tools created an integrated system that optimized the production of ceramic bricks.

2.2.2. Experimental Procedures

Raw clay samples were collected from two locations: Pliocene marl from the Akrach region and Triassic clay from the Maaziz region. Samples were named for their primary color—yellow clay and red clay—for easy identification. The clay materials were sorted to provide statistically valid samples. First, all samples were dried at 40 °C for 48 h, then characterized, and their mechanical properties were tested as ceramics.

For both raw samples, the mineralogical and physicochemical properties were identified using IR spectroscopy and X-ray fluorescence (FX). X-ray diffraction spectra (XRD) were recorded for the raw clay as well as its corresponding <2 μ m fraction (Treated). A separation of the clay fraction from the rock (bulk sample) greatly facilitates the mineralogical characterization as it minimizes contamination by non-clay minerals. Fractions <2 or <0.2 μ m, or both, are commonly separated and studied (Figure 3). To recover the fraction below 2 μ m, which is rich in clay minerals, we proceeded as follows: The first step was crushing raw rock by hand using an agate mortar. The second step was treatment of samples with hydrochloric acid to remove carbonates (CaCO₃, Ca Mg (CO₃)₂ (HClN/5) with rigorous stirring for 2 h. The carbonates were eliminated according to the following reactions (CaCO₃ + 2HCl → Ca²⁺, 2Cl⁻ + H₂O + CO₂ (g)); when the carbonates were completely dissolved, the reaction was stopped

by diluting the suspension in distilled water. The suspension was then allowed to settle in the beaker, followed by washing to remove the excess acid from the samples and allow the clays to deflocculate. In the third step, a fine fraction (grain size $< 2 \mu\text{m}$) was taken during the static sedimentation of the suspended particles according to the stock law [16]. Initial preparation of samples was performed as detailed by Ihekwe [17].

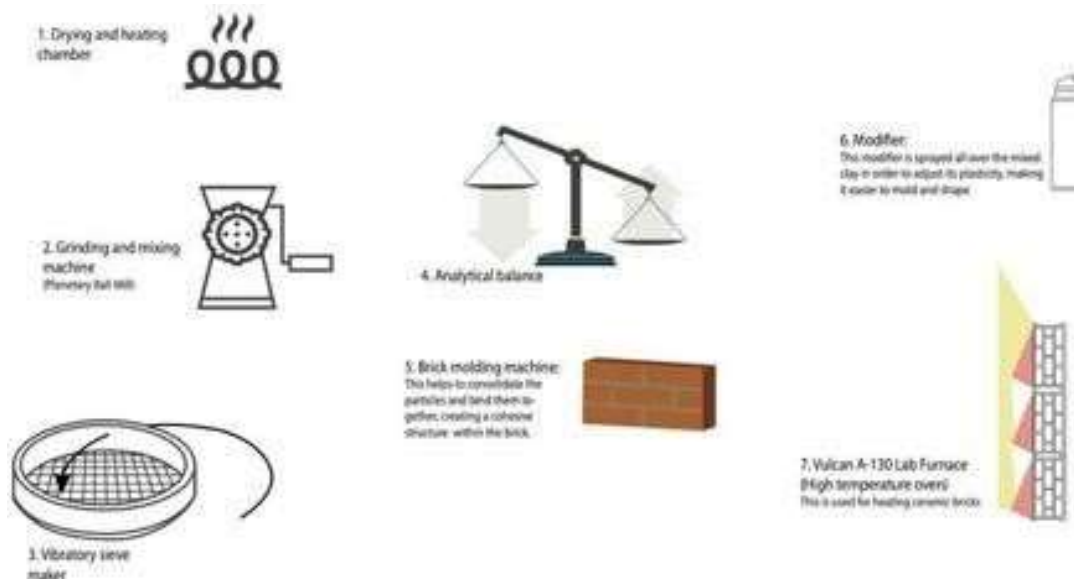


Figure 3.
Materials and equipment used to fabricate ceramics [16].

Step 1 (Fig. 4): The clay was subjected to a drying and heating chamber apparatus at a controlled temperature of $105 \text{ }^\circ\text{C}$ to facilitate the evaporation of moisture content within the clay.

Step 2 (Fig. 4): The dried clay specimens were processed using a planetary ball mill, a grinding and mixing machine, to decrease the particle size of the compact clay and enhance its overall homogeneity. The resulting clay material was then sieved using graduated sieves with apertures of 300 μm , 200 μm , and 100 μm . The fine particles with a size below 100 μm were carefully collected, while the remaining particles were discarded. The collected fine particles were subjected to corresponding measurements, using an analytical balance for precise evaluation.



Figure 4.
Steps 1 and 2 of the brick fabrication process.

Step 3 Figure 5 In total, four mixtures were prepared, starting with 100 grams of red clay (100%); we created new mixtures by reducing the amount of red clay, mixing 90 grams with 10grams of yellow marl, 80 grams with 20 grams of yellow marl, and 70 grams with 30 grams of yellow marl. These mixtures were then placed in a mold and pressed using a brick-making machine; the process was completed in just 20 seconds.

Step 4 Figure. 6 We investigated the effect of yellow marl by adding 10 grams, 20 grams, or 30 grams to the previous red clay mixtures. It was found that, while 100 grams of red clay alone tends to fracture, the addition of 10% yellow marl significantly reduces the fractures, although further additions of 20% and 30% yellow marl did not provide additional benefits. Thus, incorporating 10% yellow marl notably enhances the integrity of the red clay mixtures.



Figure 5.
Steps 3 and 4 of the brick fabrication process.

Step 5 Figure 8 The fabricated bricks were subjected to thermal processing within a dry apparatus, operating at a temperature of 105 °C, to facilitate the removal of moisture present within the bricks. The four bricks had the same size as before the high-temperature treatment. Using the rectangular cuboid formula (Equation (1)), the same volume was obtained for each sample.

$$V = l * w * h = 10\text{cm} * 5\text{cm} * 1.1\text{cm} = 55\text{cm}^3 \quad (1)$$

Step 6 Figure 8 The samples underwent heat treatment as part of the experimental procedure. The ceramic bricks were subjected to heat treatment at a temperature of 900 °C. Each brick was placed in an oven maintained at the aforementioned temperature for a period of 2 hours. This procedure was repeated for the remaining samples.

Post heat treatment, the dimensions of each brick were reevaluated. The measurements revealed a change in length and width as the percentage of yellow clay increased from 0% to 30%, while the thickness remained constant but different from the initial one.

Table 1.
Dimensions and volume of ceramic bricks after high-temperature treatment.

Clay composition		Size before high-temperature treatment				Size after high-temperature treatment			
Red clay (%)	Yellow clay (%)	Length (cm)	Width (cm)	Thickness (cm)	Volume (cm ³)	Length (cm)	Width (cm)	Thickness (cm)	Volume (cm ³)
100	0	8.9	4.4	1.0	55	1.1	0.6	0.1	39.16
90	10	9.2	4.5	1.0	55	0.8	0.5	0.1	41.4
80	20	9.3	4.6	1.0	55	0.7	0.4	0.1	42.78
70	30	9.5	4.7	1.0	55	0.5	0.3	0.1	44.65

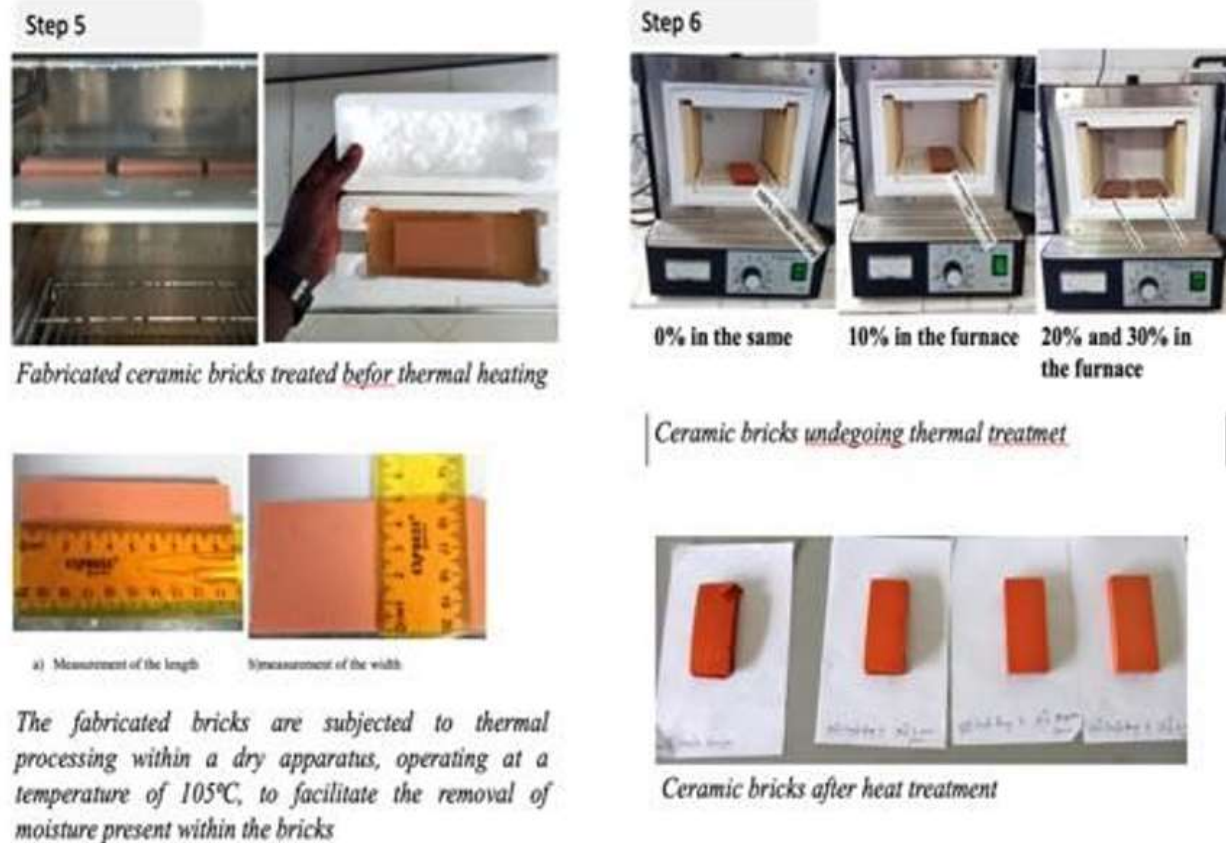


Figure 6.
Steps 5 and 6 of the brick fabrication process.

3. Results and Discussion

3.1. Mineralogical Characterizations

3.1.1. ASTER Data Treatment

ASTER data treatment was used to highlight the spatial distribution of clays in the Rabat- Salé-Kénitra region. ASTER imagery provides spatial data that help to visualize the distribution and extent of clay deposits. This spatial understanding can assist with locating areas with high clay potential, which is important for industrial applications such as ceramics, brick making, and other construction materials.

Clay rocks, including in the studied areas, are represented by dark red zones in the image; the high values on the abundance map (Fig. 9) mainly correlate with the sedimentary rocks on the geological map in Figure 2.

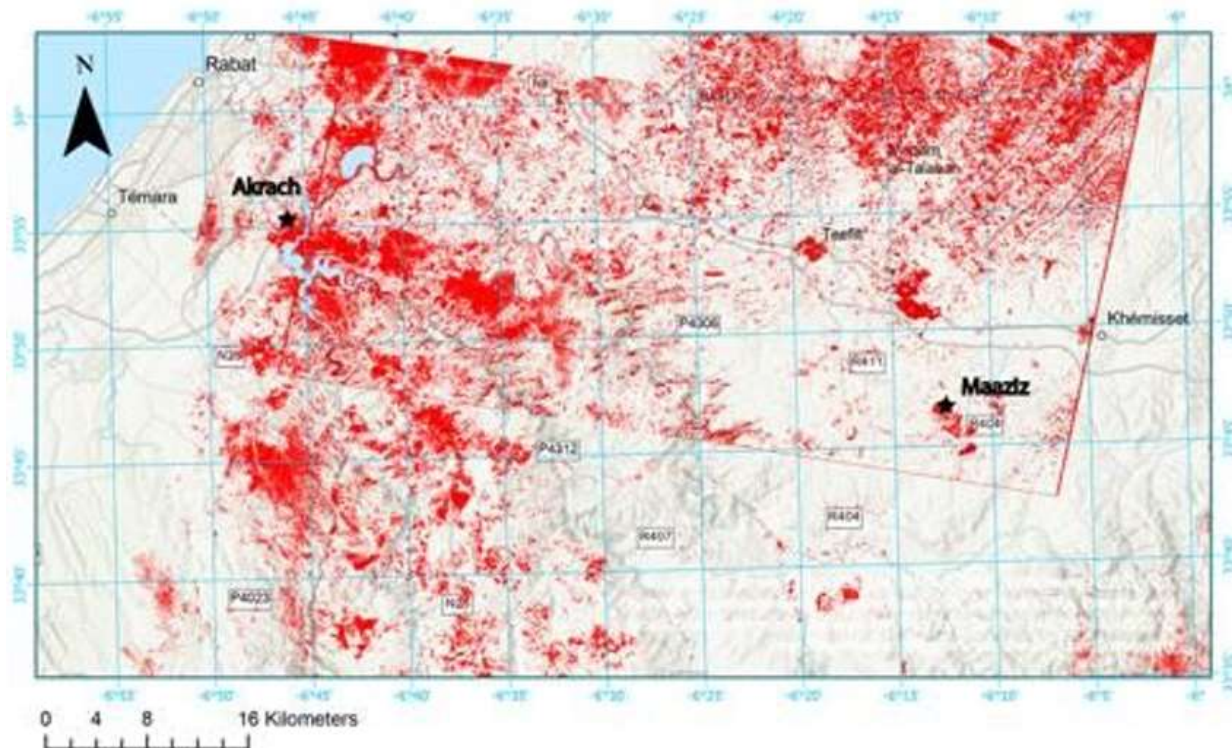


Figure 7.
Mineral occurrences in the study area after ASTER data treatment: Clay index.

3.2. X-ray Diffraction

The X-ray diffraction patterns (XRD) recorded for the yellow clay of Akrach in Figure 8 show that there were different phases. As verified by ASTM (American Society for Testing Materials) cards, we noted the presence of calcite (CaCO_3) and albite ($\text{NaAlSi}_3\text{O}_8$), characterized by peaks at 3.03 \AA (29.39° in 2θ) and 3.72 \AA (23.89° in 2θ), respectively [18] [19]. The reflection at 7.6 \AA (11.59° in 2θ) seems considerably more intense than that observed at 4.28 \AA (20.7062° in 2θ) and 3.06 \AA (29.09° in 2θ). A distance of 7.6 \AA , typical of gypsum ($\text{Ca}(\text{SO}_4) \cdot 2(\text{H}_2\text{O})$), was recorded for the red clay of Maaziz (Fig. 9). Characteristic quartz (SiO_2) peaks can be observed for both samples at $2\theta = 26.62$ corresponding to lattice distance 3.34 \AA [20]. These peaks, in particular, appear wide and less intense, which indicates that the phyllosilicates present in the raw clay have low crystallinity and their crystallites are small.

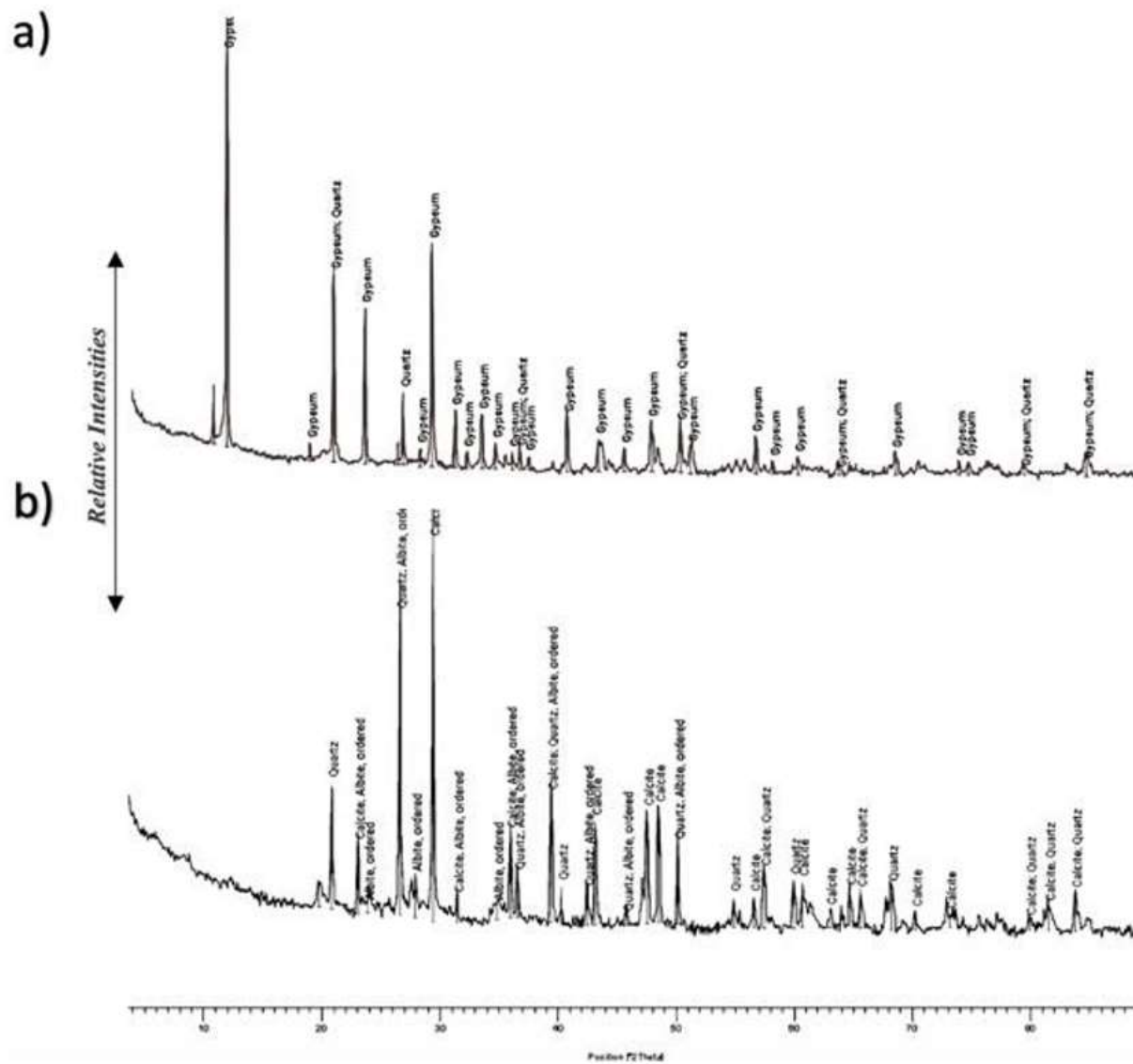


Figure 8. (a) X-ray diffraction pattern of raw red clay material. (b) X-ray diffraction pattern of raw yellow clay material.

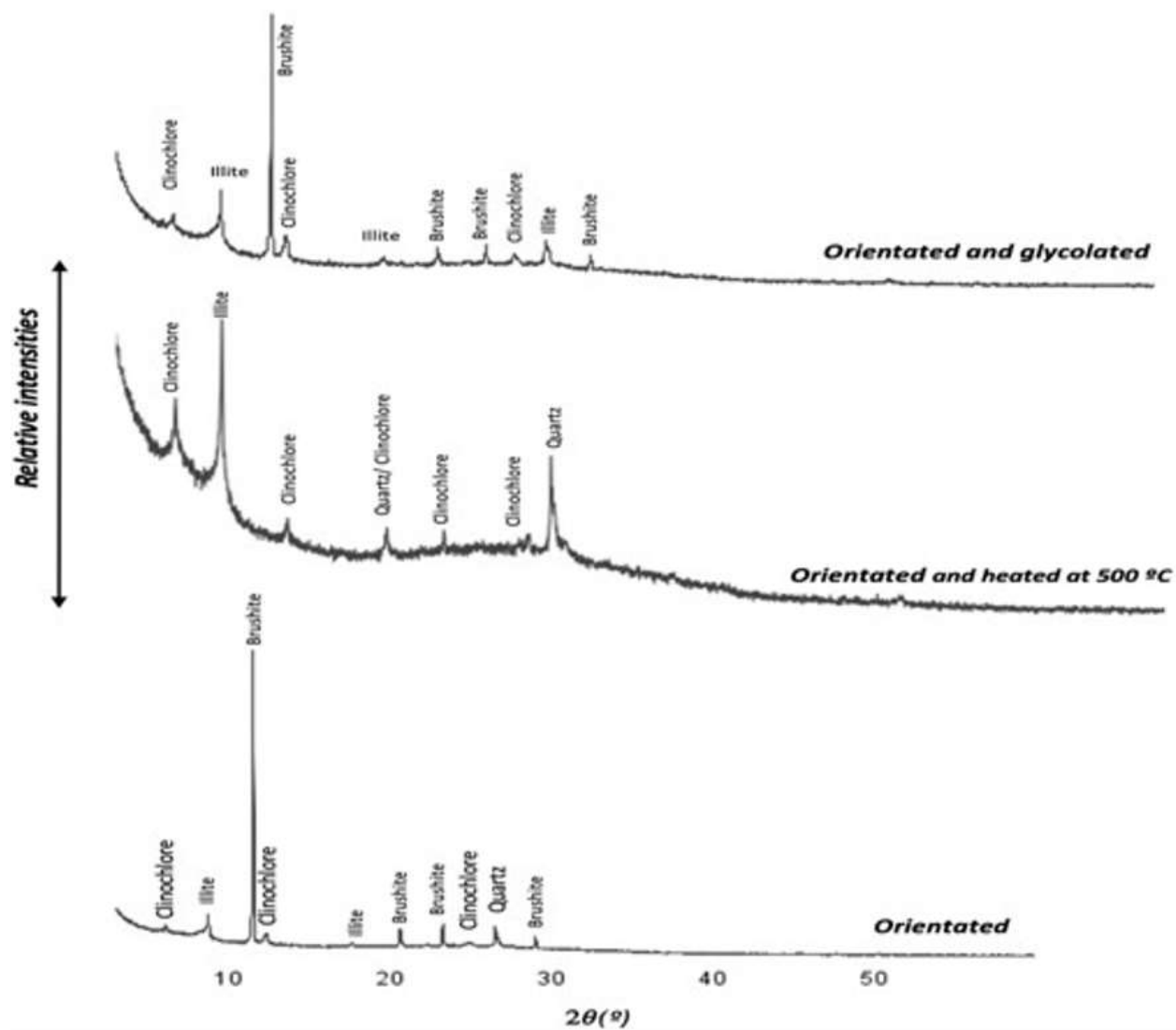


Figure 9.
X-ray diffraction pattern of the treated red clay from Maaziz.

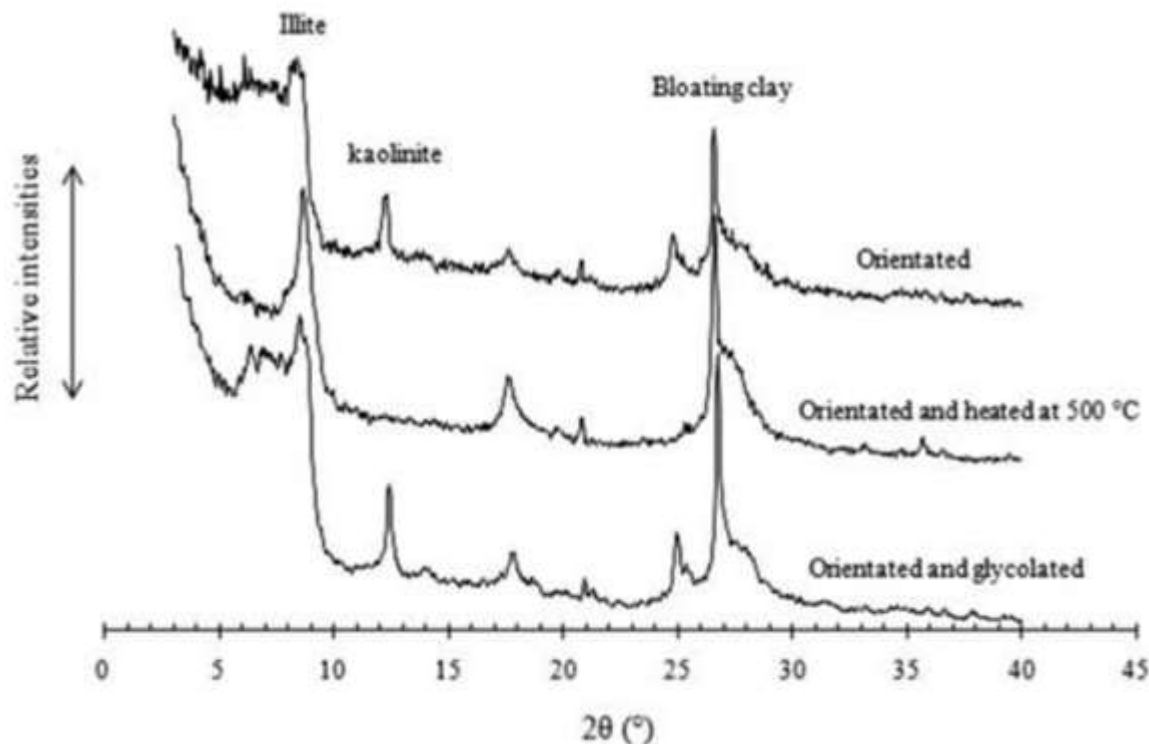


Figure 10. X-ray diffraction pattern of the yellow clay (Akrach Miocene clay) [21].

Table 2. Diagnostic X-ray diffraction peaks of treated red clay from Maaziz.

Clinochlore			Brushite		
Pos. (°2Th.)	d-spacing(Å)	Rel.int. (%)	Pos. (°2Th.)	d-spacing(Å)	Rel. Int. (%)
6.1727	14.31889	2.23	11.5808	7.64142	100.00
12.3883	7.14509	3.47	20.6719	4.29685	6.24
24.9157	3.57377	0.98	23.3195	3.81465	7.49
25.3558	3.51273	9.97	29.0429	3.07462	3.89
			47.7818	1.90356	0,37
Illite			Quartz		
Pos. (°2Th.)	d-spacing(Å)	Rel.int. (%)	Pos. (°2Th.)	d-spacing(Å)	Rel. Int. (%)
8.8105	10.03684	8.59	26.5773	3.35399	6.10
17.7228	5.00462	1.20			

Diffractograms of the fine fraction of the red clay were obtained from oriented samples (normal, glycolated, and heated) (Fig. 9). Spectral analysis of the clay from the Maaziz region indicated the presence of two very intense peaks, one corresponding to brushite and the other to illite, and two other moderately intense peaks, one corresponding to clinochlore and the other to quartz, which implies that our clay is heterogeneous. Previous studies showed that yellow clay from the Akrach region is dominated by kaolinite, illite, and blotting clay (Smectite) [21]. The clay fractions of the two samples from Maaziz and Akrach region had quartz and calcite, respectively, as major impurities. This confirms the results of the chemical analysis, which showed high proportions of SiO₂ (quartz) for red clay and

CaO₃ (calcite) for yellow clay. The results allowed us to confirm that yellow clay from the Akrach region is from a marly deposit very rich in calcite, while the red clay from the Maaziz region is part of a continental sedimentary deposit that is rich in evaporites (gypsum).

3.3. Infrared Spectroscopy

Infrared spectroscopy was used to complement the analysis of the clay sample.

The obtained spectra are illustrated in Figure 12. The broad absorption peak between 3300 cm⁻¹ and 3600 cm⁻¹ is due to O–H stretching vibration. The presence of two bands between (3526.10 cm⁻¹ and 3396.94 cm⁻¹) provides clear evidence for internal O–H stretching, also associated with the OH group structure of clinocllore [22] [23]. The band extending between 1600 and 1700 cm⁻¹ can be attributed to the valence vibrations of the OH group of adsorbed water located at 1682.85 cm⁻¹ and 1619.73 cm⁻¹ [24] [25] [26], with the greater intensity in the yellow clay sample indicating a higher anionic exchange capacity. The interlayer water absorption capacity was confirmed in yellow clay by the absorption band at 3610 cm⁻¹, which is more intense. This explains the more pronounced swelling property of this clay.

However, the absorption bands at 794.79 cm⁻¹, corresponding to quartz [27], remain observable in the red clay, but with much lower intensities than in yellow clay, in perfect agreement with the X-ray crystallographic analysis. The Si–O stretching bands at 1091.88 cm⁻¹

and 794.79 cm⁻¹, as well as the Al–O bending at 1003.26 cm⁻¹, are characteristic of aluminosilicate minerals [28].

The absorptions at 596.92, 454.54, and 434.26 cm⁻¹ observed in red clay (Fig. 12a) are due to (H–O–) P=O for acid phosphates of the brushite [29] [30].

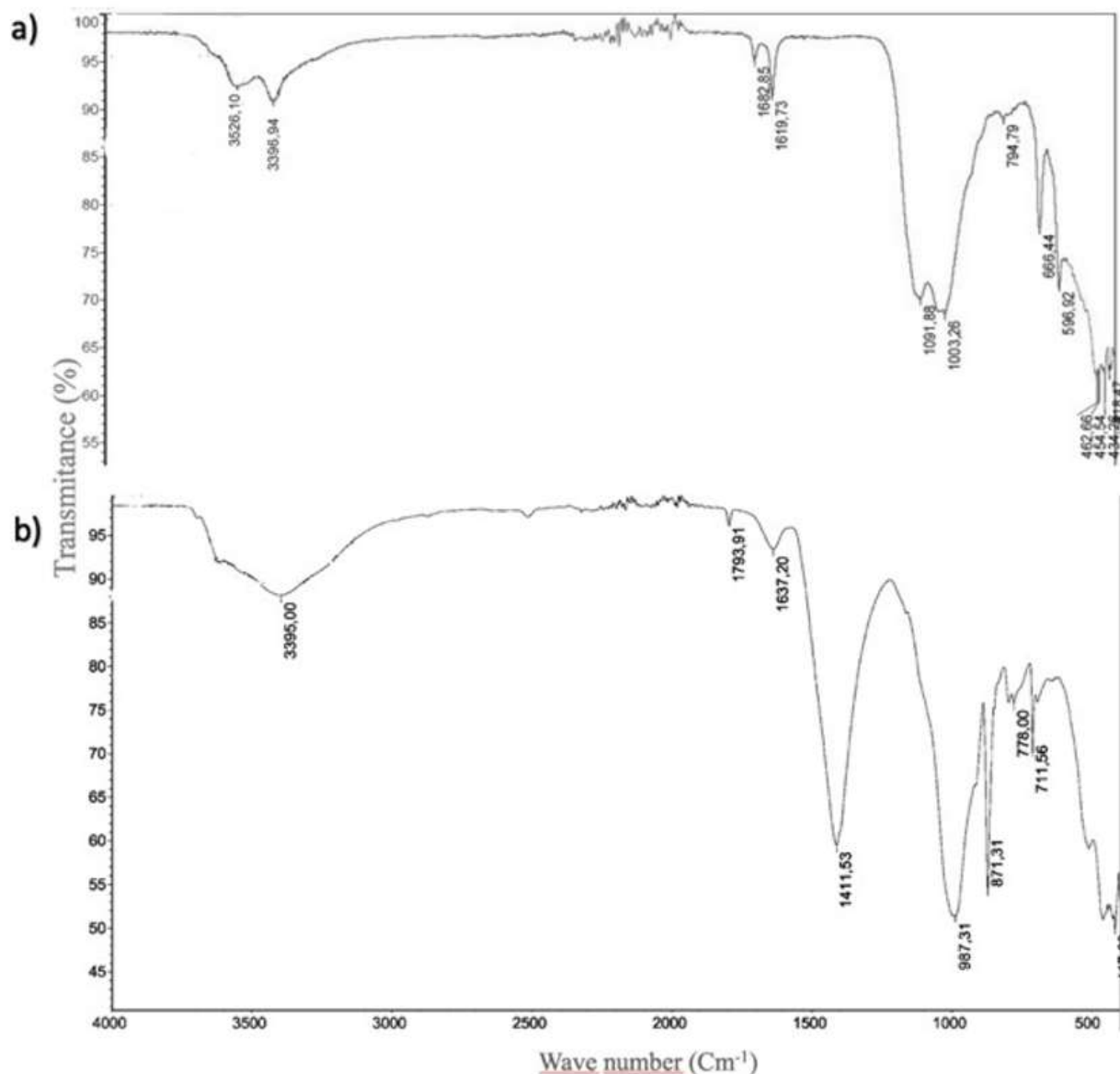


Figure 11. (a) Infrared spectrum of the red clay (Triassic clay). (b) Infrared spectrum of the yellow clay (Pliocene clay).

Table 3.
Diagnostic infrared spectroscopy spectra of raw clay of Maaziz.

Bands (cm ⁻¹)	Interpretation
3526.10	(3200-3800) cm ⁻¹ O-H/ inner hydroxyl/
3396.94	(3200-3800) cm ⁻¹ O-H/ inner hydroxyl/
1682.85	(1600-1700) cm ⁻¹ H-O-H interlayer hydroxyl
1619.73	(1600-1700) cm ⁻¹ H-O-H interlayer hydroxyl
1091.88	Quartz
1003.26	Si-O
794.79	Si-O-Al and Mg-O-H
596.92, 454.54, 434.26	(H-O-) P=O for acid phosphates

3.3.1. Chemical Analysis

The chemical compositions resulting from the X-ray fluorescence spectroscopy (FX) of theraw clay are given in Table 5.

Table 4.

Chemical composition of the two raw clay samples.

Raw red clay from Maaziz region											
Oxide	SiO ₂	CaO	Al ₂ O ₃	Fe ₂ O ₃	MgO	Na ₂ O	ClO	K ₂ O	P ₂ O ₅	SO ₃	
Concentration (%)	14.34	19.60	5.566	1.421	2.665	0.07878	0.03812	0.7528	0.04675	36.16	
Oxide	O	S	Ca	Si	Al	Mg	Fe	K	Na	Cl	P
Concentration (%)	53.14	14.48	14.01	6.702	2.946	1.607	0.994	0.624	0.058	0.038	0.020
Raw yellow clay from Akrach region											
Oxide	SiO ₂	CaO	Al ₂ O ₃	Fe ₂ O ₃	MgO	Na ₂ O	ClO	K ₂ O	P ₂ O ₅	SO ₃	
Concentration (%)	31.74	24.55	9.392	2.237	2.227	2.101	1.452	1.036	0.2823	0.1741	
Oxide	O	S	Ca	Si	Al	Mg	Fe	K	Na	Cl	P
Concentration (%)	48.70	0.0697	17.54	14.83	4.971	1.343	1.565	0.8602	1.559	1.452	0.123

The percentages of silica and aluminum were high, which indicates the presence of phyllosilicates in both samples. High calcium (24.55%) therefore indicates that the yellow clay of Akrach is rich in calcite (CaCO₃), while high levels of sulfur (36.16%) were linked to the presence of gypsum in red clay.

These analyses revealed the presence of potassium, which is a load balancer and may be present in the leaf interlayer of illite. The chemical analysis results were generally in agreement with the DRX results for the raw material.

The alumina/silica ratio provides information about the permeability of the material with respect to humidity; the greater the ratio, the greater the permeability [31]. In our study, the ratio was smaller in yellow clay (red clay: Al₂O₃/SiO₂ = 0.38; yellow clay: Al₂O₃/SiO₂ = 0.29). This low value was in agreement with the DRX results, which recorded the peaks of bloating clay in the treated clay spectra.

3.3.2. Physical Properties of Ceramics

In this experimental investigation, after the ceramic brick specimens were subjected to heat treatment, their weight was determined and denoted as the dry mass (msec).

The ceramic brick samples were immersed in water for approximately 30 minutes to facilitate water infiltration. After this time, the samples were removed from the water and wiped lightly with a cotton rag to remove any excess water from the surface. The saturated mass (msat) was determined.

The ceramic brick specimens were then suspended by a string and weighed while immersed in water; this weight was recorded as the suspended mass (mh) Table 6.

Table 5.

Masses obtained after heat treatment, water saturation, and suspension.

Specimens (%)	Dry Mass, msec(g)	Saturated Mass, msat(g)	Mass suspended on water, mh(g)
0	50.88	54.85	31.45
10	52.60	58.29	31.94
20	83.16	94.42	49.49

30	88.02	98.03	50.47
----	-------	-------	-------

Based on the above results, the porosity, water absorption, and apparent density of the fabricated ceramic bricks were calculated.

Porosity (P%) was calculated by
 absorption (A%) by
 density (Dap) by

$$\frac{m_{sat} - m_{sec}}{m_{sat} - m_h} \quad \text{(Equation (2))},$$

$$\frac{m_{sat} - m_{sec}}{m_{sec}} \quad \text{(Equation (3))},$$

$$\frac{m_{sec}}{m_{sat} - m_h} \quad \text{(Equation (4))}.$$

The calculated parameters are shown in the table below.

Table 6.

Calculations of porosity, water absorption, and apparent density.

Specimens (%)	Dry mass, msec (g)	Humid mass, msat (g)	Mass in suspension, mh (g)	P: Porosity %	A: Water Absorption n %	Apparent density (g/cm ³)
0	50.88	54.85	31.45	16.97	7.80	2.17
10	52.6	58.29	31.94	21.60	10.81	1.99
20	83.16	94.42	49.49	25.06	13.54	1.85
30	88.02	98.03	50.47	21.05	11.37	1.85

3.4. Effect of Additional Yellow Clay

Based on these observations, several characteristics can be concluded regarding the study of the ceramic bricks. The use of pure red clay was found to consistently result in brittle bricks that broke easily. This suggests that, while red clay contains beneficial minerals such as gypsum, illite, brushite, and chlorite (clinochlore is part of the chlorite group), which contribute to thermal stability and enhance the overall plasticity of the clay mixture, it may lack the necessary strength or cohesiveness when used alone. The mineral composition plays a significant role in determining the mechanical properties of the final ceramic product.

This brittleness is likely influenced by the amount of gypsum present in red clay, as shown by the DRX results (Fig. 8a) and the chemical composition (SO₃ = 36.16%) (Table 4), which is known to decompose upon heating. The decomposition of gypsum can lead to the release of steam and gas, creating internal pressures that contribute to fracture development during the firing process. The instability introduced by the gas release can compromise the integrity of the bricks [32].

Previous studies have shown that the decomposition of gypsum, as analyzed using thermogravimetric analysis (TGA), begins around 150 degrees Celsius, confirming that significant mass losses occur at temperatures commonly associated with the firing process. This mass loss can lead to structural weaknesses in the final product if not properly accounted for [33].

In addition to the effects of gypsum, we also considered the impact of uneven local water loss during the drying process. If certain areas of the clay body dried faster than others, this could lead to differential shrinkage and ultimately create weaknesses in the material. However, our observations indicate that, while drying-induced cracks can occur, they were not the primary cause of the fractures observed after firing. Instead, we found that the interaction between residual moisture and the decomposition of gypsum played a more critical role during the firing stage. This highlights the importance of controlling both moisture content and the thermal profile during firing to mitigate fracture risks.

The introduction of yellow clay into the red clay mixture significantly improved the durability of the resulting bricks. The most notable enhancement was observed at a proportion of 20-30% yellow clay, which suggests that this specific ratio optimizes the balance between plasticity and strength. The minerals

present in yellow clay, such as illite, smectite and kaolinite, are known for their high plasticity. This may enhanced plasticity allows the clay to deform more easily under stress without cracking [34], resulting in a composition that did not break during the manipulation and molding process.

The interaction between red and yellow clays appears to create a synergistic effect that enhances the overall structural integrity of the bricks. This interaction implies that the unique properties of both clays work together to form a more cohesive and resilient material. For instance, the presence of illite and chlorite (chlinochlore) in both clays may improve the physical properties of the ceramics, such as plasticity, workability, and firing behavior [34]. Kaolinite, being an aluminosilicate, provides a substantial source of aluminum oxide upon firing, which can lead to a more robust ceramic structure. This enhancement in Al_2O_3 content not only contributes to improved physical properties but also plays a role in the esthetic qualities of the fired ceramic, influencing its color and finish [35] [36].

Additionally, the primary clay minerals, such as quartz and calcite, contribute to the overall properties of the materials. Quartz enhances the mechanical strength and thermal stability of the ceramic products [37], while the high calcite content in yellow clay acts as a fluxing agent during firing, promoting better densification through the transformation into calcium oxide (CaO) and formation of a glassy phase at higher temperatures. Although complete vitrification and the maximum enhancement of these properties generally occur at higher temperatures (around 1000 °C or more), the decomposition of calcite at 900 °C can still have beneficial effects on the initial properties of ceramic materials [38].

3.5. Volume

The ceramic brick samples with 0%, 10%, 20%, and 30% yellow clay all started with the same volume of 55 cm³. After heating, their volumes changed: 39.1 cm³ for 0%, 41.4 cm³ for 10%,

42.78 cm³ for 20%, and 44.65 cm³ for 30%. These changes show that heating affected the samples. While it seems like the volumes increased, this actually means that the samples with yellow clay shrank less than samples without it. Therefore, the addition of yellow clay influenced how much the ceramic bricks shrank during heating (Table 7). Yellow clay, which contains minerals such as smectite and calcite, can enhance plasticity and moisture retention. As a result, bricks made with yellow clay tend to shrink less compared to those made with only red clay. This means that, while all samples experience some shrinkage during firing, the presence of yellow clay leads to reduced overall shrinkage, contributing to a more stable volume in the final product.

3.6. Porosity

Looking at the data, we notice that the porosity generally increases as the percentage of marking increases from 0 to 20 and then decreases at 30, as seen in the table below. This suggests that there might be an optimal range for the yellow clay percentage that leads to desirable porosity levels (Table 6).

3.7. Water Absorption

The four samples were marked as 0, 10, 20, and 30, representing different percentages of yellow clay. The corresponding water absorption values for these samples were 7.80%, 10.81%, 13.54%, and 11.37%, respectively, as shown in the table below. From these results, we observe a clear trend: as the marking percentage increases, the water absorption of the ceramic bricks also increases. The sample marked 0 had the lowest water absorption of 7.80%. This indicates that the porosity of the ceramic materials increases as the marking percentage increases (Table 6).

3.8. Density

From the data obtained, it is observed that, as the sample number increases (from 0 to 30), the apparent density decreases. This suggests that the samples become less dense and likely have a higher porosity. However, we noted that the apparent densities of samples 20 and 30 were the same (1.85) in

the table below. This indicates that these two samples have similar apparent densities despite having different percentages marked (20 and 30). This could suggest that the porosity reached a maximum or that other factors beyond the marking percentage influenced the apparent density.

The increase in water absorption and porosity of fired pottery samples after adding yellow clay is primarily due to the presence of minerals like smectite and calcite. Smectite enhances water retention and plasticity, resulting in greater porosity [39]. Additionally, calcite decomposes during firing, producing gases that create voids, leading to a more porous structure [40]. As porosity increases, the volume of open pores rises, which directly contributes to a decrease in density. The relationship between porosity and density is inverse; as one increases, the other typically decreases.

4. Conclusions

The experimental techniques employed in this study effectively revealed the phyllite and mineral phases, as well as the physicochemical parameters of the analyzed clays. The findings indicate the presence of two distinct clay types, each with unique mineralogical, chemical, and structural properties.

Akrach clay is characterized by a predominance of quartz, clay minerals (smectite, illite, and kaolinite), and carbonates (calcite). Its alumina/silica ratio suggests a high absorption capacity and low porosity, contributing to its plasticity. In contrast, Maaziz clay exhibits an abundance of quartz and gypsum, alongside clay minerals (brushite, illite, and chlorite). This clay has a lower absorption capacity, resulting in reduced plasticity.

The results of this study can facilitate the pre-characterization of exploited clay minerals commonly used in traditional ceramic fabrication. Various tests conducted with these two geomaterials aimed to promote their application in traditional ceramic brick manufacturing, yielding the following conclusions:

Several tests were carried out using these two geomaterials in order to promote them in the field of traditional ceramic brick manufacturing. The results were as follows:

Thermal heating significantly influenced the volume changes of the ceramic brick samples.

The volume of the samples increased with higher percentages of Akrach clay, indicating that its inclusion promoted the expansion or swelling of the ceramic bricks during heating.

Porosity generally increased with the percentage of Akrach clay from 0% to 20%, before decreasing at 30%, suggesting an optimal range for achieving desirable porosity levels.

The water absorption of the traditional ceramic bricks increased with elevated percentages of Akrach clay, with the sample containing 0% Akrach clay exhibiting the lowest water absorption. This confirms that porosity increases with higher clay percentages.

The apparent density of the samples decreased as the clay percentage increased from 0% to 30%, indicating a correlation between higher porosity and lower density.

Overall, these findings underscore the importance of carefully selecting the proportion of clay to optimize the properties of ceramic bricks, balancing aspects such as shrinkage, porosity, water absorption, and density for enhanced performance.

While the addition of yellow clay solved some issues related to fracture, the resulting high water absorption and porosity, along with low bulk density, suggest that these ceramics may not be suitable for structural applications where strength is critical. However, they can be beneficial in several fields, including:

- Filtration: The porous nature allows for the effective removal of impurities in water or air filtration systems [41]
- Insulation: High porosity and low density contribute to thermal insulation properties, making them useful in insulating materials. [42]
- Artistic Ceramics: These ceramics can be utilized in artistic applications where texture and aesthetics are prioritized over mechanical strength. [Lightweight Building Materials: The low density can be advantageous in construction, particularly where reduced weight is beneficial. [43]
- Soil Amendments: High porosity ceramics can improve soil aeration and water retention in

agricultural applications. [44]

The preliminary results suggest that raw clay from the Akrach and Maaziz regions may be suitable for ceramic applications. The Pliocene marl deposit and Triassic red clay deposit represent valuable sources of raw geomaterials that could be utilized in ceramic production, thereby promoting sustainability in the Rabat-Salé-Kénitra region.

Author Contributions: S.L. conceptualized the study, performed the data analysis, and wrote the manuscript. S.E.K., C.L.A., and I.K. performed laboratory tasks. S.E.K. and A.A. prepared the original draft. B.B., N.E.M., M.S., and M.E.J. reviewed and edited the paper. M.E.J. was responsible for the software. All authors have read and agreed to the published version of the manuscript.

Acknowledgments: The authors would like to thank the Solids Laboratory of the National Center for Technical and Scientific Research and the Geomaterials Laboratory of the Scientific Institute.

Copyright:

© 2024 by the authors. This article is an open access article distributed under the terms and conditions of the Creative Commons Attribution (CC BY) license (<https://creativecommons.org/licenses/by/4.0/>).

References

- [1] K. BERRAD, M. El Youssi & Sanae B., 2022. Inventorying Rabat-Salé-Kénitra Region's Geological Heritage Within Central Morocco: A Useful Tool for Developing Regional Geotourism Activity Original Article Published: 08 August 2022 Volume 14, article number 91, (2022).
- [2] Y .El Hafiane, & M .ElGhorfi. Ceramic production in Rabat-Salé-Zemmour-Zaer region (Morocco): Technological study and cultural heritage. *Journal of Archaeological Science: Reports*, 20, 108-115. 2018
- [3] I. Rodica-Mariana, F. Radu-Claudiu , S. Sofia , Irina F., S. Raluca , C. Canu Chapter: Ceramic Materials Based on Clay Minerals in Cultural Heritage Study. In book: *Clays, Clay Minerals and Ceramic Materials Based on Clay Minerals* (pp.159- 184) 2016. DOI:10.5772/61633.
- [4] M. El Ghorfi & Y. El Hafiane. Traditional ceramics in the region of Rabat-Salé- Zemmour-Zaer (Morocco): Technological study and cultural heritage. *Journal of Cultural Heritage*, 14(6), e165-e171. 2013
- [5] M. Laila, E. Omar, L. Mohamed, J.Raouf. *Geomaghreb* n°7, 2011, pp. 13-20. Characterization of Miocene Marls from the Fes Region before and after Doping with Manganese Oxide (MnO₂) e.g. (in French) 2011
- [6] M. El Halim , L. Daoudi, M. El Ouahabi, J.Amakrane, N.Fagel. *Materials and Environmental Sciences* ISSN: 2028-2508 CODEN: JMESC Mineralogy and firing characteristics of clayey materials used for ceramic purposes from Sale region (Morocco). 2018.
- [7] Hicham N., Ali A., Kamal E., Abdelilah E and Meriam E. 2019. Characterization of Neogene marls from the Kert Basin (northeast Morocco): suitability for the ceramics industry. Published online by Cambridge University Press: 04 November 2019
- [8] Mondher H., Walid H., Bechir M., Mounir M., F. Rocha J.A. L., Fakher J., 2012. Production of ceramic bodies from Tunisian Cretaceous clays *March 2012 Clay Minerals* 47(1):59-68.
- [9] Baghdad A., Bouazi R., Bouftouha Y., Bouabsa L., Fagel N. 2017. Mineralogical characterization of Neogene clay areas from the Jijel basin for ceramic purposes (NE Algeria -Africa) *Science*. Volume, February 2017, Pages 176-183.
- [10] Hassan E., Abdelfatah T., Ayoub EL M., Omar S., Fernando SI., Francisco G. L., Antonio A., David M., Mounia T & Jesus D.L. R. D. 2014. Geodynamic setting context of the Permian and Triassic volcanism in the northwestern Moroccan Meseta from petrographical and geochemical data. *Bulletin de l'Institut Scientifique, Rabat, Section Sciences de la Terre*, 2014, n° 36, 55-67.
- [11] Et-Touhami M., 1996. L'origine des accumulations salifère du trias Marocain :apport de la geochimie du Brom du sel du bassin de Khemisset (Maroc central). *Geomaterials/sedimentology/geochemistry*. C.R.Acad. Sci. Paris, t.323, serie Iia, p.591 à 598, 1996.
- [12] El Kasmi S., Zriouil M., Ahmamou M and Barka N. 2016. Physico-chemical and mineralogical characterization of clays collected from Akrach region in Morocco. *J. Mater. Environ. Sci.* 7 (10) (2016) 3767-3774 ISSN: 2028-2508.
- [13] Ben Mlih A., Laadila M., El kochri A., El youssi M., 2004. Le remplissage synrift au permien et au trias du bassin de Tahanaout (Haut Atlas de Marrakech, Maroc) géodynamique et organisation sédimentaire. December 2004. *Estudios Geológicos* 60(3-6). DOI:10.3989/egol.04603-685.
- [14] Mashimbye Z.E., Clercq W.P & Van N.A. 2012. "Using Landsat ETM+ data to identify and map potential saline soil areas in the Berg River catchment area. Western Cape. South Africa". *South African Journal of Plant and Soil*. 29(2).

- 97-103.
- [15] Rowan. L.C. & Mars. J.C. (2003). "Lithologic mapping in the Mountain Pass. California area using Advanced Spaceborne Thermal Emission and Reflection Radiometer (ASTER) data". *Remote Sensing of Environment*. 84(3). 350-366
- [16] Aghris S., Laghrib F., Koumya Y., El Kasmi S., Azaitraoui M., Farahi A., Sajieddine M., Bakasse M. 2021. Exploration of a New Source of Sustainable Aluminosilicate Clay Minerals from Morocco: Mineralogical and Physico-Chemical Characterizations for Clear Upcoming Applications. *Journal of Inorganic and Organometallic Polymers and Materials* <https://doi.org/10.1007/s10904-021-01950-1>
- [17] Ihekwe G. O., Josiah N.S., Kingsley O., Godwin M.K., Iheoma C.N., Peter A.O. 2020.Characterization of certain Nigerian clay minerals for water purification and other industrial applications. *Heliyon* 6(4): e03783. DOI:10.1016/j.heliyon. 2020. e03783.
- [18] Salam K. Mustapha H. Lahcen B., Saadia A., Mohamed E. A., Christophe. 2017. Spectrometric characterization of marbles from Morocco: provenance study. D.Pittaluga, F. Fratini (eds.), *Conservation and promotion of architectural and landscape heritage of the Mediterranean coastal sites*, ed. F. Angeli, Milano, 2017, p.121.
- [19] Aditya K., Himanshu S., ameer K. T., Param G., 2016.New Occurrence of Albitite from Nubra Valley, Ladakh: Characterization from Mineralogy and Whole Rock Geochemistry. *Current Science* 111(9):1531-1535.
- [20] Qlihaa A., Dhimmi S., Melrhaka F., Hajjaji N., Srhiri A.2016. Physico-chemical characterization of a Moroccan clay. *J. Mater. Environ. Sci.* 7 (5) (2016) 1741-1750
- [21] El Kasmi S., Lahrich S., Farahi A., Zriouil M., Ahmamou M., Bakasse M., ElMhammedi M.A., *J. Taiwan Inst. Chem. Eng.* 58 (2015) 165.
- [22] Min Y., Meifang Y., Haihui H., Guangli R., Ling H., Zhuan Z.2018.Near-Infrared Spectroscopic Study of Chlorite Minerals. *Journal of Spectroscopy* 2018(1):1-11 DOI: 10.1155/2018/6958260.
- [23] Schroeder, P.A. (2002) *Infrared Spectroscopy in clay science: In CMS Workshop Lectures, Vol. 11, Teaching Clay Science*, A. Rule and S. Guggenheim, eds., The Clay Mineral Society, Aurora, CO, 181-206
- [24] ZeBilo P., Ndjeumi C.C., Mouthe A.G.A., Maicaneanu A.S., Sieliechi J. M., Kamga R.2023. Crystallochemical Properties of Natural and Modified Clays from Maroua-Cameroon Used in Water Treatment Processes. *International Journal of Engineering Research and Applications* ISSN: 2248-9622, Vol. 13, Issue 1, January 2023, pp. 139-150.
- [25] Tuddenham W.M and Lyon R.P.,1960. Infrared Techniques in the Identification and Measurement of Minerals. *Anal Chem.* 32 (1960)1630.
- [26] Frost R.L., Makó E., Kristóf J., Horváth E., Klopogge J.T., 2001. Mechanochemical Treatment of Kaolinite. *Colloid Interface Sci.* 239 (2001) 458). e.
- [27] Vijayaragavan R., Mullainathan S., Balachandramohan M., Krishnamoorthy N., Nithiyantham S., Murugesan S., Vanathi V., 2012. Mineralogical Characterization Studies on Unburnt Ceramic Product Made from Rock Residue Additives by FT-IR Spectroscopic Technique. *International Journal of Modern Physics: Conference Series* Vol. 22 (2013) 62–70. DOI: 10.1142/S2010194513009938.
- [28] Aarfane A., Salhi A., El Krati M., S. Tahiri, Monkade M., Lhadi E.K., Bensitel M.2012. *J. Mater. Environ. Sci.* 5 (6) (2014) 1928.
- [29] Madhurambal G., Subha R and Mojumdar S.C.2009. "Crystallization and Thermal Characterization of Calcium Hydrogen Phosphate Dihydrate Crystals," *Journal of Thermal Analysis and Calorimetry*, Vol. 96, No. 1, 2009, pp. 73-76. doi:10.1007/s10973-008-9841-1.
- [30] Rajendran K., and Dale Keefe C., 2010. "Growth and Characterization of Calcium Hydrogen Phosphate Dihydrate Crystals from Single Diffusion Gel Technique," *Crystal Research and Technology*, Vol. 45, No. 9, 2010, pp. 939945. doi:10.1002/crat.200900700]. Brushite
- [31] [31] Jarraya I., Fourmentin S., Benzina M., 2010. Adsorption de cov par un matériau argileux tunisien organomodifié. *J. Soc. Chim. Tun.* 12 (2010) 139.
- [32] [32] Charola A.E. . Josef P., Michael S., 2007.Gypsum: A review of its role in the deterioration of building materials. *Environmental Earth Sciences*.
- [33] Karim G .w., Hugi. E., wullschleger. L. Frank .TH., 2007. Gypsum Board in Fire Modeling and Experimental Validation. May 2007. *Journal of Fire Sciences* 25(3):267-282. DOI:10.1177/0734904107072883.
- [34] Neeraj. Kand Chandra. M., 2021. Basics of Clay Minerals and Their Characteristic Properties. *Clay and Clay Minerals*.
- [35] Ammar. TK.,2022. Effect of Aluminum Oxide on the Mechanical Properties of ceramic crucibles prepared by slip casting from local kaolin clay material while smectite contributes to increased plasticity. *Texas Journal of Engineering and Technology* ISSN NO: 2770-4491 <https://zienjournals.com>.
- [36] Youssef .C., Ali .Br., Faouzi .M and Ezzedine. S.,2021. Characterization, thermal behaviour and firing properties of clay materials from Cap Bon Basin, north-east Tunisia, for ceramic applications. Published online by Cambridge University Press: 28January 2021.
- [37] Swapan Kr Das et al, 2004.Shrinkage and strength behaviour of quartzitic and kaolinitic clays in wall tile compositions April 2005. *Applied Clay Science* 29(2): 137-143.DOI : 10.1016/j.clay.2004.10.002.
- [38] M. Melhem. 2024.The Effect of Calcite Additives on Clay for Ceramic Tile Manufactory. *Qualicer* 2024. 5 y 6 de marzo – castelló (españa)

- [39] Thamyres C. C., Camila N. M., Margarita. B., E. Hildebrando, Roberto F. N and Francisco R. Valenz. 2019. Ceramic Properties: Clay Smectite Synthetic. The Minerals, Metals & Materials Society 2019. https://doi.org/10.1007/978-3-030-05749-7_49
- [40] Giuseppe C., Carlos R. N. Eduardo S., Olga C., Maria Jose D. L. T.,. May 2001. Carbonate and Silicate Phase Reactions during Ceramic Firing. European 13(3):621- 634 DOI: 10.1127/0935-1221/2001/0013-0621
- [41] P. Sanjiv Kanade, Someshwar .S. B, Introduction to Water Worldin A Guide to Filtration with String Wound Cartridges, 2016
- [42] A. Chen et al. Enhancing thermal insulation and mechanical strength of porous ceramic through size-graded MA Hollow Spheres. Ceramics International. <https://doi.org/10.1016/j.ceramint.2023.08.033>. 2023.
- [43] S. Siengchin. A review on lightweight materials for defence applications: Present and future developments, in Defence Technology, 2023.
- [44] M. Mohammed Amer& I. Hachem. IMPACT OF SOME SOIL AMENDMENTS ON PROPERTIES AND RODUCTIVITY OF SALT AFFECTED SOILS AT KAFR EL-SHEIKH GOVERNORATE. Egyptian Journal of Soil Science. DOI: 10.21608/ejss.2018.2356.1148.2018